

# Various Mechanisms of ULF Wave–Electron Interaction: Case Studies



Maksim A. Chelpanov, Olga S. Mikhailova, Pavel N. Mager, Ekaterina E. Smotrova, and Dmitri Yu. Klimushkin

**Abstract** Two case studies of ultra-low frequency (ULF) wave–electron interaction are presented. In both cases, the eastward propagating Alfvén wave with strong poloidal component was generated via drift resonance with energetic electrons, but the generation mechanisms were different: kinetic instability in one case and alternating current caused by movement of the electron cloud in the other. In the first case, the Van Allen Probe data were examined. The poloidal Alfvén wave was found simultaneously with 38 keV electrons injected into magnetosphere during a substorm onset. It was found that the wave was generated through an instability caused by the strong radial inhomogeneity of electron density (the gradient instability). In the second case, the wave was found in the MMS spacecraft data. The wave also was in the drift resonance with the particles, but the conditions for plasma instability were not satisfied. In this case, we arrive at a conclusion that the wave was apparently generated through the moving source mechanism, that is, by an alternating current created by a drifting substorm-injected electron cloud.

**Keywords** ULF waves · Wave–particle interaction · Plasma instability

## 1 Introduction

Ultra-low frequency (ULF) waves are regularly observed in the magnetosphere. Waves with high azimuthal wavenumbers  $m$  are known to interact with energetic particles in the magnetosphere [1]. Two generation mechanisms of the high- $m$  ULF waves were suggested. The first one involves resonance with energetic particle population resulting in energy transfer from particles to wave and kinetic instability developing [2, 3]. The other supposes generation by an azimuthally drifting particle cloud (moving source) as proposed in [4, 5]. Within this concept substorm-injected particles represent an alternating current, which can be a source for Alfvén waves [6, 7].

---

M. A. Chelpanov (✉) · O. S. Mikhailova · P. N. Mager · E. E. Smotrova · D. Yu. Klimushkin  
Institute of Solar-Terrestrial Physics, Irkutsk, Russia  
e-mail: [max\\_chel@iszf.irk.ru](mailto:max_chel@iszf.irk.ru)

Signatures of ULF waves–particle interactions are found in the spacecraft data, and a large body of evidence on drift and drift-bounce resonance with energetic particles is accumulated. In most observational cases ULF waves interact with westward-drifting protons. Recent observational data gave evidences for both generation mechanisms by protons: instability [8–11] and moving source [12]. The drift resonance with electrons can be experienced by eastward propagating waves. However, such wave represents no more that 10% of events [13, 14]. Therefore, wave interactions with electrons have been studied less. To our knowledge, the process of wave generation by energetic electrons have not been observed yet.

In this paper, we examine two observational cases to show two different wave generation mechanisms associated with substorm-injected electrons. In the first case a wave was generated by a gradient instability. In the second case the plasma instability condition was not satisfied, although the drift resonance was also confirmed. The probable generation mechanism in this case can apparently be described by the moving source theory.

## 2 Data Analysis

### 2.1 Case 1. The ULF Wave Generation by an Electron Cloud Spatial Gradient

A Pc4 ULF wave was registered in the prenoon magnetosphere at a distance of about  $6 R_E$  from the Earth on 27 October 2012 by Van Allen Probes A. The wave had a duration of 45 min and an amplitude of 0.7 nT. Its frequency was 10 mHz. The wave had a mixed polarization: the amplitudes of the poloidal (radial)  $b_r$  and toroidal (azimuthal)  $b_a$  components differed slightly. We used the 4 s data from the Electric and Magnetic Field Instrument Suite for and Integrated Science (EMFISIS) [15] and the 11 s data from the Electric Fields and Waves (EFW) instrument [16] to study oscillations in the electric field. To study oscillations in electron fluxes, 11 s data from the Magnetic Electron Ion Spectrometer (MagEIS) instrument were used [17]. The ULF wave was observed outside the plasmasphere on the background of the recovery phase of a substorm ( $Kp = 10$ ,  $Dst = -20$  nT). The event was preceded by a number of substorms. One of the substorms was registered  $\sim 70$  min before the start of the event (onset time 0314UT), with the AL index reaching  $\sim -150$  nT. It is likely that this substorm was a source of energetic electrons responsible for the generating the observed ULF wave.

The MagIES instrument registered the electron cloud at a time of the wave observation (Fig. 1). We found resonant oscillations coinciding in frequency with the oscillations in the electric field (Fig. 2). The noticeable modulations were at two energy channels, 38 and 58 keV, with the at the energy of 38 keV. The maximum amplitude was recorded for the particles with  $90^\circ$  pitch angles which corresponds to the fundamental (symmetrical relative to the equator) harmonic of the wave and the

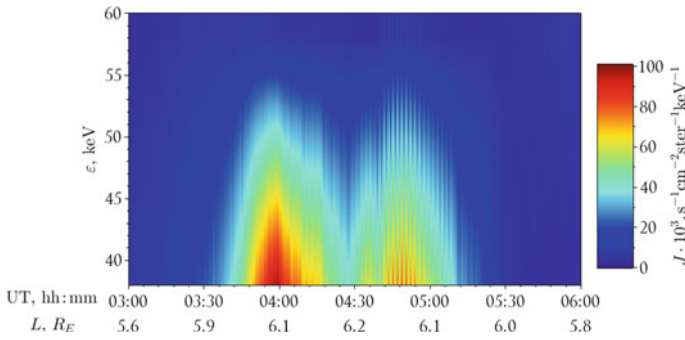


**Fig. 1** The spectrogram of the electron differential flux  $J$  for energies  $\varepsilon$  from 38 to 60 keV and pitch angle  $\alpha = 90^\circ$

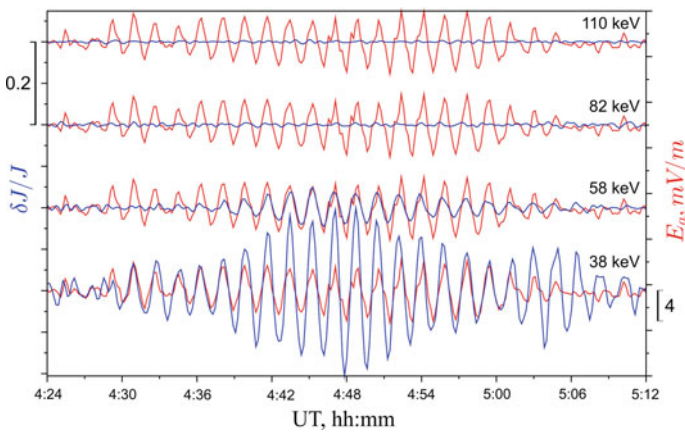


**Fig. 2** The relative electron flux oscillations  $\delta J/J$  for different energies (blue), where  $\delta J$  and  $J$  are perturbed and unperturbed fluxes, respectively, and the azimuthal component of the electric field  $E_a$  (red), filtered in Pc4 range. One can see the null phase shift between  $E_a$  and  $\delta J/J$  oscillations for the 38 keV flux, which corresponds to the drift resonance. The phase shift between  $E_a$  and  $\delta J/J$  oscillations for the 58 keV flux is  $5^\circ$

drift resonance [3, 18]. Moreover, the phase shift between azimuthal component of electric field ( $E_a$ ) and the 38 keV electron modulation was close to zero. We also calculated the phase shift between  $E_a$  and the 58 keV electron flux modulations. It is  $5^\circ$ , which means that the 58 keV electrons are ahead of the observed wave. Therefore, we conclude that the energy 38 keV is the resonant one.

There are three standard ways to calculate the azimuthal wavenumber  $m$ . The first is to calculate the phase shift between the magnetic field oscillations at two or more satellites. The second one is the method of gyrophases. The third way is to infer  $m$  from the drift resonance condition [19]. In our case we were able to use the third way.

The drift resonance condition is

$$\omega - m\omega_d = 0, \quad (1)$$

where  $\omega$  is the wave frequency,  $m$  is the azimuthal wave number, and  $\omega_d$  is the angular frequency of the particle magnetic drift averaged over the bounce period. Based on (1), the azimuthal wavenumber was of the order of 110–115. That is, it was an azimuthally small-scale wave moving eastward. The azimuthal wavelength  $\lambda_a$  is approximately 2200 km, i.e. about  $0.3R_E$ .

In order the amplitude of the wave to increase, i.e. to transfer energy from particles to the wave, it is necessary to have an unstable distribution of particles in energy (inverse energy distribution function) or in space (the presence of a sharp radial gradient of the distribution function) [20]. For the instability to develop, it is necessary the condition to be met

$$\hat{Q}F = \left[ \frac{\partial F}{\partial \varepsilon} + \frac{m}{\omega} \frac{c}{q B_{eq} L} \frac{\partial F}{\partial L} \right]_{\varepsilon_{res}} > 0. \quad (2)$$

Here  $F$  is the distribution function,  $\varepsilon$  is the particle energy,  $q$  is the particle charge,  $c$  is the speed of light,  $B_{eq}$  is the magnetic field at the geomagnetic equator,  $L$  is the McIlvaine parameter used as the radial coordinate, and  $\varepsilon_{res}$  is the resonant energy. Condition (2) will be satisfied either at  $\partial F/\partial \varepsilon > 0$  or at  $\partial F/\partial L < 0$ . In our case, the second inequality is satisfied. This means that the wave must be generated by the spatial gradient instability. The condition  $\partial F/\partial L < 0$  is met. The electron distribution had a negative spatial gradient from 0400UT to 0427UT. This implies that the radial gradient instability resulted in generating the wave. We should note that the radial gradient is calculated using a single spacecraft data. We assume that the azimuthal displacement of the satellite is small compared to the radial one. Temporal variations are also not taken into account.

We suggest that the wave was generated by a steep radial gradient in the electron number density caused by the electron injection into the magnetosphere during a substorm. Using the electron flux data and the AL index data, we determined the location of the substorm that was a source for the electron cloud. The estimation shows that the substorm onset occurred at 0314UT. It was localized at about 00 MLT.

## 2.2 Case 2. The ULF Wave Generation by an Electron Cloud as a Moving Source

The Magnetospheric Multiscale (MMS) Mission is a constellation of four closely located spacecraft [21]. Their mutual position is used to reveal the spatial properties of a ULF wave registered on 7 July 2020. We used data on the magnetic field provided by the MMS Fluxgate Magnetometer [22] in slow survey mode (sampling rate 8/s). The Energetic Ion Spectrometer (EIS) data from the Energetic Particle Detector (EPD) investigation [23] were used for the electron flux analysis. The spacecraft were in the 3.6–3.7 MLT sector. They moved towards the Earth at distances 13–11  $R_E$ . The oscillations were being recorded in the magnetic field from 0815UT for about 45 min. The frequency varied within 3–4 mHz (Pc5 range). At first, the radial and azimuthal components had roughly the same magnitudes ( $\sim 2$  nT) with a weaker compressional component (up to 1 nT). During the wave registration period, the azimuthal to radial component ratio was increasing, and the wave was transforming to a predominantly toroidal pulsation.

The crosswavelet transform of the radial magnetic field components at spacecraft pairs were used to calculate the azimuthal wavenumber [24]. A phase of  $W_i(\omega, \tau)W_j^*(\omega, \tau)$  at the wave frequency represents a phase difference  $\Delta\phi_{ij}$  between two spacecraft. Here,  $W_i$  and  $W_j^*$  are the wavelet transform and the complex conjugate wavelet transform for signals at two spacecraft, respectively, at the frequency  $\omega$  and the time shift  $\tau$ . Knowing the phase shifts and spatial coordinate differences in the GSE coordinate system for three spacecraft pairs, we calculated wavelengths along each axis. After transforming the wavelength components to a coordinate system referenced to a local magnetic field, we revealed an azimuthal wavenumber. It varied from +23 to +27. This implies that the wave was propagating to the east in the azimuthal direction, and it was azimuthally small-scale. As it was mentioned, such waves can effectively interact with energetic electrons.

The wave was registered during quiet geomagnetic conditions. The Dst index values had been above  $-15$  nT during previous 24 h. The vertical component of the interplanetary magnetic field changed its direction several times before the event (from 23 UT on 6 July 2020 to 07 UT on 7 July 2020). A substorm was registered during the wave observation period, with the SML index of about  $-200$  nT at 0730UT. A cloud of energetic electrons was apparently injected during this substorm.

An increase in the energetic electron population was also registered at the MMS spacecraft (Fig. 3). The electron fluxes at several energy ranges were modulated with the wave frequency. The relative flux  $\delta J/J$  of the 89 keV electrons featured the highest modulation magnitude (Fig. 4). Moreover, the phase difference between  $\delta J/J$  for the 89 keV electrons and the radial magnetic field component oscillation was about  $90^\circ$  at the wave frequency, whilst the fluxes at other energies had different phase shifts relatively to the magnetic field oscillations. These facts point at the drift resonance similar to the previous case.

According to the drift resonance condition, the wave and particle parameters should satisfy relation (1). However, with the wave frequency of 3.2 mHz and

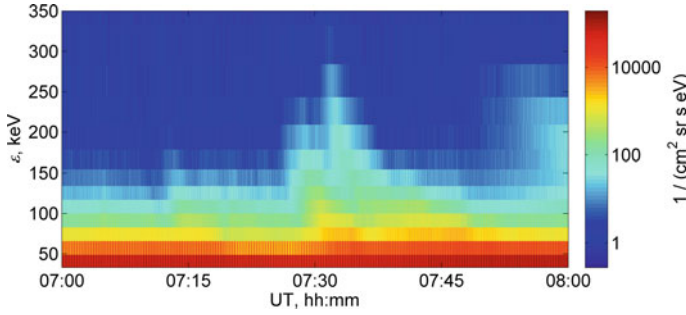


**Fig. 3** The spectrogram of the electron differential flux  $J$  for energies  $\varepsilon$  from 33 to 319 keV on 07 July 2020

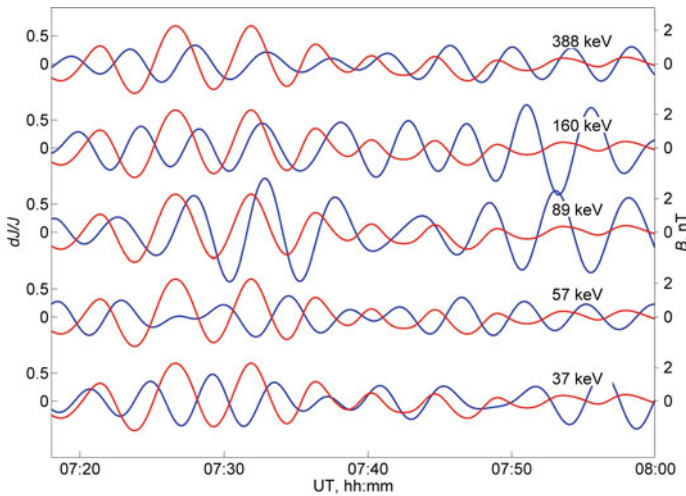


**Fig. 4**  $\delta J/J$  for five energy ranges (blue); the radial component of the magnetic field filtered in the Pc5 range (red). Phase difference between these parameters is different for various particle energies, and it is close to  $90^\circ$  at 89 keV

azimuthal wavenumber  $m = +25$ , the angular velocity of the resonant particles should be  $0.8 \cdot 10^{-3}$  rad/s. This value corresponds to electron energy of about 40 keV. This is more than two times lower than the resonant energy seen in the observation.

The wave was observed at large L-number in the nightside magnetosphere, where the field differs substantially from a dipole. Therefore, the most probable reason for the above discrepancy is the deviation of the magnetic field from the dipole form. Relations (1) and (2) are not applicable for such conditions, and a deviation could affect the particle angular frequency calculation as the wave phase velocity can have a strong non-azimuthal component. Indeed, the calculation show that the wave had comparable azimuthal and radial (inward) wavelengths of order of  $2\text{--}2.5 \cdot 10^3$  km.

To estimate the drift velocity in the non-dipole magnetic field we calculated the spatial gradient of the magnetic field using the radial separation of the spacecraft pairs. Implying that the pitch angle is close to  $90^\circ$ , the drift velocity

$$\mathbf{u}_d = \frac{\varepsilon c}{qB} \left[ \mathbf{e}_\parallel \times \frac{\nabla \mathbf{B}}{B} \right], \quad (3)$$

where  $q$  is the electron charge,  $B$  is the magnetic field magnitude,  $\mathbf{e}_\parallel$  is the unit vector along the magnetic field line, and  $\nabla \mathbf{B}$  is the magnetic field gradient. Relation (3) is valid when the effect of field line curvature is small as the pitch angle is  $\sim 90^\circ$ . For the 89 keV electrons in this case the drift velocity is directed to the east in the azimuthal direction and away from the Earth in the radial direction, with an absolute value  $u_d = 5-6 \cdot 10^5$  m/s.

For the non-dipole case, a general form of relation (1) should be used:

$$\omega - \mathbf{k} \mathbf{u}_d = 0, \quad (4)$$

where  $\mathbf{k}$  is the wavenumber. The radial component of  $\mathbf{k}$  was negative, i.e., the wave propagated to the east and towards the Earth. The angle between  $\mathbf{k}$  and  $\mathbf{u}_d$  was below  $90^\circ$ , and relation (4) was satisfied during the event meaning that the drift resonance occurred.

Similar to the above case, we investigated the conditions for the plasma instability leading to the wave generation. For the gradient or the bump-on-tail instability the relation should be met:

$$\frac{\hat{Q}F}{F} = \left[ \frac{1}{F} \frac{\partial F}{\partial \varepsilon} + \frac{1}{\omega} \frac{c}{qB} [\mathbf{k}_\perp \times \mathbf{e}_\parallel] \cdot \frac{\nabla F}{F} \right]_{\varepsilon_{res}} > 0. \quad (5)$$

However, condition (5) was not met, and  $\hat{Q}F/F$  was below 0 during the wave registration period.

The estimations show that while the ULF wave gained energy through the drift resonance with the substorm-injected energetic electrons, a plasma instability was not a generation mechanism for the wave. The alternative mechanism for the wave generation is the emitting Alfvén high- $m$  waves by an alternating current representing a cloud of drifting charged particles [6]. Such mechanism was suggested by [4] for the magnetosphere framework. Later it was elaborated in [5, 7]. According to the theory, a wave is observed simultaneously with a particle cloud, and it propagates in the direction of the particle drift.

### 3 Discussion and Conclusion

We analysed the data for two ULF wave observation cases related to interaction with energetic electrons. Case 1 was registered with the Van Allen Probes spacecraft A, and case 2 was registered with the MMS spacecraft.

For case 1, we reported the first observation of a resonant generation of an ULF wave by an electron cloud in the magnetosphere. We assume that the electrons were injected into the magnetosphere during a substorm. At the same time with the wave registration, modulations in the fluxes of energetic electrons were observed. We found modulations at the frequency of the observed wave in several energy channels. It is shown that these modulations are caused by the drift resonance of electrons with an energy of 38 keV. The wave is a fundamental harmonic of the Alfvén mode with an azimuthal wavenumber  $m \sim 110\text{--}115$  propagating to the east. It was established that the ULF wave was generated through the gradient instability due to a steep density gradient.

In case 2 a cloud of energetic electrons was also registered simultaneously with the eastward-propagating ULF wave. The wave propagation was not exclusively azimuthal and had a considerable radial component. However, it is shown that the drift resonance occurred. The main difference to the previous case was the absence of a condition for the wave generation by a plasma instability. For the generation mechanism the theory of the moving source was proposed. This theory can explain some features of wave–particle interaction that are typically seen in observations. They include a narrow range of observed azimuthal wave numbers and a coincidence in the azimuthal direction of particle drift and wave phase propagation. In theory, a wave generated by a moving source can have a distinguishing feature: it can transform from a toroidal wave into a poloidal one, and then modify back to a toroidal pulsation. This requires a certain spatial distribution of energetic particles which does not always develop [7]. Without this condition it is apparently impossible to distinguish a wave generated by a moving source. Therefore, in case 2 we assume such mechanism as the wave-generating plasma instability threshold was not overpassed.

**Acknowledgements** The work was financially supported by the Ministry of Science and Higher Education of the Russian Federation. We acknowledge the NASA Van Allen Probes and Craig Kletzing for use of EMFISIS data, John Wygant for use of EFW data, Bernard Blake for use of ECT/MagEIS data, Roy B. Tober for use of the FGM data from MMS, and Barry H. Mauk for use of the EDP EIS MMS data.

### References

1. D.Y. Klimushkin, P.N. Mager, M.A. Chelpanov, D.V. Kostarev, *Solar-Terrestrial Physics* **7**(4), 33–66 (2021). <https://doi.org/10.12737/stp-74202105>
2. A.B. Mikhailovskii, O.A. Pokhotelov, *Soviet Journal of Plasma Physics* **1**, 786 (1975)
3. D.J. Southwood, *Journal of Geophysical Research* **81**, 3340 (1976). <https://doi.org/10.1029/JA081i019p03340>



4. N.A. Zolotukhina, *Issled. geomagn. aeron. i fiz. Solntsa* (in Russian) **34**, 20 (1974)
5. A.V. Guglielmi, N.A. Zolotukhina, *Issled. geomagn. aeron. i fiz. Solntsa* (in Russian) **50**, 129 (1980)
6. A.I. Akhiezer, I.A. Akhiezer, R.V. Polovin, A.G. Sitenko, K.N. Stepanov, *Plasma electrodynamics. Vol. 1: Linear theory* (International Series of Monographs in Natural Philosophy, Vol. 68, Pergamon Press, Oxford, UK., 1975)
7. P.N. Mager, D.Y. Klimushkin, *Annales Geophysicae* **26**, 1653 (2008). <https://doi.org/10.5194/angeo-26-1653-2008>
8. C. Wei, L. Dai, S.P. Duan, C. Wang, Y.X. Wang, *Earth and Planetary Physics* **3**(3), 190 (2019). <https://doi.org/10.26464/epp2019021>
9. K. Yamamoto, M. Nose, K. Keika, D.P. Hartley, C.W. Smith, R.J. MacDowall, L.J. Lanzertotti, D.G. Mitchell, H.E. Spence, G.D. Reeves, J.R. Wygant, J.W. Bonnell, S. Oimatsu, *Journal of Geophysical Research: Space Physics* **124**(12), 9904 (2019). <https://doi.org/10.1029/2019JA027158>
10. O. Mager, *Journal of Geophysical Research: Space Physics* **126**(11), e2021JA029241 (2021). <https://doi.org/10.1029/2021JA029241>
11. A.V. Rubtsov, O.S. Mikhailova, P.N. Mager, D.Y. Klimushkin, J. Ren, Q.G. Zong, *Geophysical Research Letters* **48**, e2021GL096182 (2021). <https://doi.org/10.1029/2021GL096182>
12. N.A. Zolotukhina, P.N. Mager, D.Y. Klimushkin, *Annales Geophysicae* **26**, 2053 (2008). <https://doi.org/10.5194/angeo-26-2053-2008>
13. P.T.I. Eriksson, A.D.M. Walker, J.A.E. Stephenson, *Advances in Space Research* **38**, 1763 (2006). <https://doi.org/10.1016/j.asr.2005.08.023>
14. M.A. Chelpanov, P.N. Mager, D.Y. Klimushkin, O.V. Mager, *Solar-Terrestrial Physics* **5**, 51 (2019). <https://doi.org/10.12737/stp-51201907>
15. C.A. Kletzing, W.S. Kurth, M. Acuna, R.J. MacDowall, R.B. Torbert, T. Averkamp, D. Bodet, S.R. Bounds, M. Chutter, J. Connerney, D. Crawford, J.S. Dolan, R. Dvorsky, G.B. Hospodarsky, J. Howard, V. Jordanova, R.A. Johnson, D.L. Kirchner, B. Mokrzycki, G. Needell, J. Odom, D. Mark, R. Pfaff, J.R. Phillips, C.W. Piker, S.L. Remington, D. Rowland, O. Santolik, R. Schnurr, D. Sheppard, C.W. Smith, R.M. Thorne, J. Tyler, *Space Science Reviews* **179**, 127 (2013). <https://doi.org/10.1007/s11214-013-9993-6>
16. J.R. Wygant, J.W. Bonnell, K. Goetz, R.E. Ergun, F.S. Mozer, S.D. Bale, M. Ludlam, P. Turin, P.R. Harvey, R. Hochmann, K. Harps, G. Dalton, J. McCauley, W. Rachelson, D. Gordon, B. Donakowski, C. Shultz, C. Smith, M. Diaz-Aguado, J. Fischer, S. Heavner, P. Berg, D.M. Malsapina, M.K. Bolton, M. Hudson, R.J. Strangeway, D.N. Baker, X. Li, J. Albert, J.C. Foster, C.C. Chaston, I. Mann, E. Donovan, C.M. Cully, C.A. Cattell, V. Krasnoselskikh, K. Kersten, A. Breneman, J.B. Tao, *Space Science Reviews* **179**, 183 (2013). <https://doi.org/10.1007/s11214-013-0013-7>
17. J.B. Blake, P.A. Carranza, S.G. Claudepierre, J.H. Clemmons, W.R. Crain Jr., Y. Dotan, J.F. Fennell, F.H. Fuentes, R.M. Galvan, J.S. George, M.G. Henderson, M. Lalic, A.Y. Lin, M.D. Looper, D.J. Mabry, J.E. Mazur, B. McCarthy, C.Q. Nguyen, T.P. O'Brien, M.A. Perez, M.T. Redding, J.L. Roeder, D.J. Salvaggio, G.A. Sorensen, H.E. Spence, S.Y. Zakrzewski, M.P. Zakrzewski, *Space Science Reviews* **179**, 383 (2013). <https://doi.org/10.1007/s11214-013-9991-8>
18. D.J. Southwood, M.G. Kivelson, *Journal of Geophysical Research* **87**, 1707 (1982). <https://doi.org/10.1029/JA087iA03p01707>
19. Q.G. Zong, R. Rankin, X. Zhou, *Reviews of Modern Plasma Physics* **1**(1), 10 (2017). <https://doi.org/10.1007/s41614-017-0011-4>
20. D.J. Southwood, J.W. Dungey, R.J. Etherington, *Planetary and Space Science* **17**, 349 (1969). [https://doi.org/10.1016/0032-0633\(69\)90068-3](https://doi.org/10.1016/0032-0633(69)90068-3)
21. J.L. Burch, T.E. Moore, R.B. Torbert, B.L. Giles, *Space Sciences Reviews* **199**, 5 (2016). <https://doi.org/10.1007/s11214-015-0164-9>
22. R.B. Torbert, C.T. Russell, W. Magnes, R.E. Ergun, P.A. Lindqvist, O. LeContel, H. Vaith, J. Macri, S. Myers, D. Rau, J. Needell, B. King, M. Granoff, M. Chutter, I. Dors, G. Olsson, Y.V. Khotyaintsev, A. Eriksson, C.A. Kletzing, S. Bounds, B. Anderson, W. Baumjohann,

- M. Steller, K. Bromund, G. Le, R. Nakamura, R.J. Strangeway, H.K. Leinweber, S. Tucker, J. Westfall, D. Fischer, F. Plaschke, J. Porter, K. Lappalainen, *Space Science Reviews* **199**(1), 105 (2016). <https://doi.org/10.1007/s11214-014-0109-8>
23. B.H. Mauk, J.B. Blake, D.N. Baker, J.H. Clemmons, G.D. Reeves, H.E. Spence, S.E. Jaskulek, C.E. Schlemm, L.E. Brown, S.A. Cooper, J.V. Craft, J.F. Fennell, R.S. Gurnee, C.M. Hammock, J.R. Hayes, P.A. Hill, G.C. Ho, J.C. Hutcherson, A.D. Jacques, S. Kerem, D.G. Mitchell, K.S. Nelson, N.P. Paschalidis, E. Rossano, M.R. Stokes, J.H. Westlake, *Space Science Reviews* **199**(1), 471 (2016). <https://doi.org/10.1007/s11214-014-0055-5>
24. A. Grossman, J. Morlet, *SIAM J. Math. Anal.* **15**(4), 723-736 (1984). <https://doi.org/10.1137/0515056>